Programmed Polyene Cyclization Enabled by Chromophore Disruption

Megan M. Solans, Vitalii S. Basistyi, James A. Law, Noah M. Bartfield, and James H. Frederich*

Department of Chemistry and Biochemistry, Florida State University, Tallahassee, Florida 30326, United States

Supporting Information Placeholder

ABSTRACT: A versatile polyene cyclization strategy was developed that exploits conjugated *β*-ionyl derivatives. Photomediated disruption of the extended π-system within these chromophores unveils a contra-thermodynamic polyene that engages in a Heck-type cyclization to afford [4.4.1]-propellanes. The connectivity of overbred polycycles generated from this process is controlled by the position of the requisite C–Br bond. Thus, compared to conventional biomimetic polyene cyclization, this approach allows for complete control of regiochemistry and facilitates incorporation of both electron-rich and electron-deficient (hetero)aryl groups. This strategy was successfully applied to the total synthesis of taxodione and salviasperanol, two isomeric abietane-type diterpenes that previously could not be prepared along the same synthetic pathway.

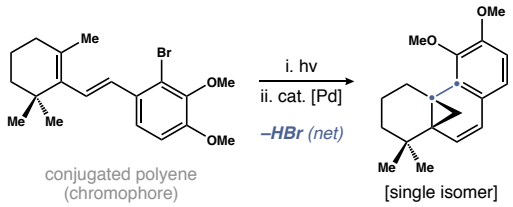

Diterpenes are a rich source of biologically active molecular scaffolds.[1,2] Members of this family harboring a fused [6-6-6] carbocyclic nucleus have gained significant attention for their valuable pharmacological profiles.[3–5] This subgroup of natural products includes abietane, pimarane, and kaurane diterpenes, which all share copalyl diphosphate as a common biosynthetic progenitor (Figure 1).[6] Although the skeletal diversity of these diterpenes is localized within the C-ring, each motif is further differentiated through late-stage oxidative tailoring.[7] This added layer of complexity hinders the design of unified synthetic entry to this diverse collection of targets. Recent advances in synthetic biology have streamlined entry to this subgroup from more accessible terpenoid starting points.[8] In contrast, polyene cyclization provides a generalized platform for *de novo* diterpene synthesis. This bioinspired strategy seeks to reorganize isolated polyenes (**1**) to polycycles (**2**) through a series of concerted C–C bond formations.[9] Both cationic and radical reaction modalities are known, as are enantioselective adaptations catalyzed by Lewis acids,[10] organocatalysts,[11] and transition metals.[12] The outcomes of polyene cyclization are predictable and governed by explicit aspects of alkene stereochemistry and electronics.[9a] This powerful feature is often exploited in total synthesis;[9c] however, it also makes it difficult to extend this strategy to diversified substrates (e.g. **1a**–**1c**) that deviate from biogenic isoprenoid precursors.[13,14]

Inspired by the photobiology of vitamin A, we envisioned a different polyene cyclization strategy. In place of isolated polyene **1**, we targeted conjugated *β*-ionyl derivative **3**. Following Buchi's investigations on the photoisomerization of *β*-ionone to *Z*-retro-γ-ionone,[15] we reasoned that diene **4** could be unveiled from **3** *via* a photoinduced [1,5]-hydride shift. The bifurcated π-systems in **4** could then be connected *via* a Heck cyclization, where the position of the C–X bond would guide site-specific incorporation of the aryl ring. We predicted that a 6-exo-trig pathway to generate alkyl metal species **A** would be favored,[16] thereby providing an avenue to modify the oxidation-state of C20, most directly by cyclization to propellane **5**. Fragmentation of this overbred species was viewed as handle for skeletal editing. Moreover, this sequence would allow **5** to be assembled from interchangeable fragments. We expected these features to not only expedite entry to diterpene natural products, but also simplify the design of tailored compositions

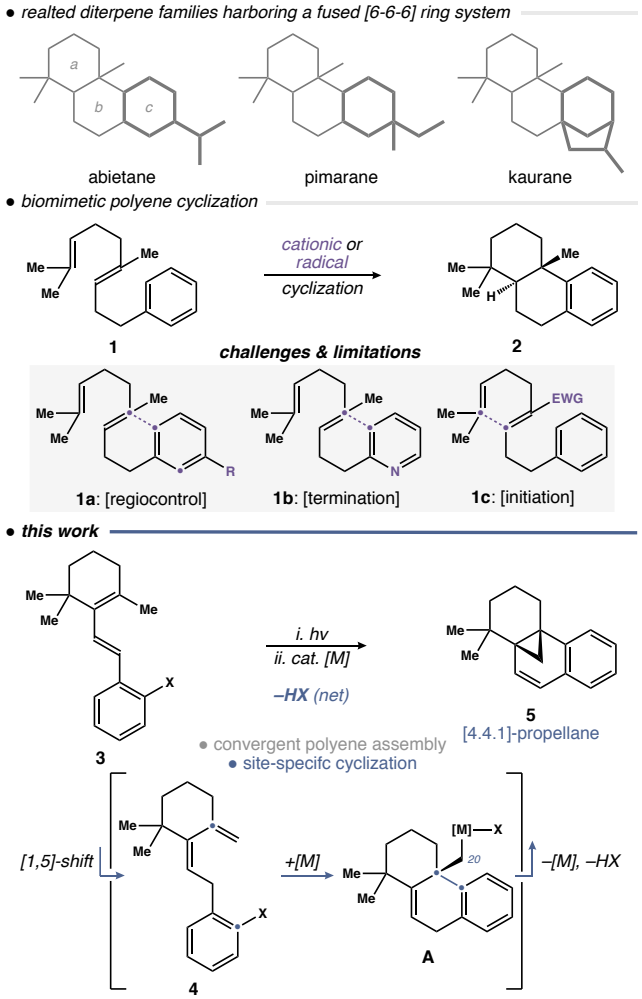

Figure 1. A polyene cyclization strategy enabled by photoinduced disruption of the extended π-system within **3**.

of matter that are beyond the reach of semi-synthesis. Herein, we report the successful implementation of this programmed polycyclization strategy and highlight its utility for the synthesis of canonical and rearranged abietane diterpenes.[17]

Table 1. Photoisomerizaiton of β-ionyl derivatives **3**.[a,b]

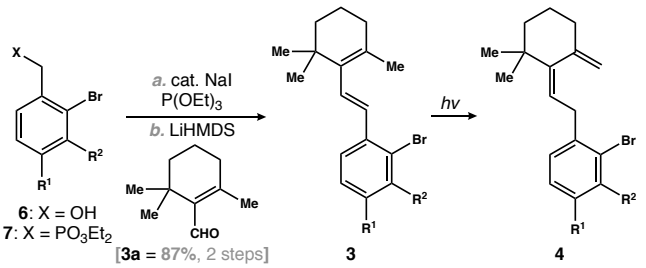

entry	solvent [0.04 M]	*hv* (nm)[c]	**3**	R^1	R^2	% of **4** (time, h)
1	THF	350	**3a**	OMe	OMe	90 (9 h)
2	THF	300	**3a**	OMe	OMe	92 (1 h)
3	THF	254	**3a**	OMe	OMe	10 (1 h)
4	dioxane	300	**3a**	OMe	OMe	93 (2 h)
5	MeCN	300	**3a**	OMe	OMe	85 (1 h)
6	dioxane[d]	300	**3a**	OMe	OMe	87[e] (5 h)
7	dioxane[d]	300	**3b**	H	H	90[e] (5 h)
8	dioxane[d]	300	**3c**	CF_3	H	86[e] (5 h)

[a] Yields were determined by ^{1}H NMR using Me_2SO_2 as an internal standard. [b] Solvent was degassed by successive freeze-pump-thaw cycles. [c] Reactions were carried out in a Rayonet photoreactor maintained at 35 °C. [d] [**4**] = 0.2 M. [e] Isolated yield after purification by silica gel chromatography.

We began by examining the photoisomerization of β-ionyl derivatives **3**. While the photosensitized geometric isomerization of β-ionyl species is established,[18] positional alkene isomerization *via* a [1,5]-hydride shift is an underexplored pathway observed upon direct irradiation.[19] Thus, it was not clear if this reaction would be broadly synthetically useful. To address this concern, a set of electronically differentiated photosubstrates **3** were prepared from benzylic alcohols **6** *via* conversion to aryl phosphonates **7** and olefination with β-cyclocitral.[20] As shown in Table 1, we were pleased to find that irradiation of **3a** (R^1, R^2 = OMe) with 350 nm light in deoxygenated THF provided *Z*-diene **4a** in 90% yield (entry 1).[21] The reaction time was reduced to 1 h using 300 nm light (entry 2). In contrast, 254 nm light resulted in decomposition (entry 3). Dioxane and MeCN gave similar results to THF (entries 4 and 5); however, the reaction rate slowed as the concentration of **3a** increased. Guided by these observations, we developed a general procedure using 300 nm light in dioxane (0.2 M) that provided **4a** in 87% yield after 5 h (entry 6). This transformation was remarkably efficient, with no evidence of other products by ^{1}H NMR. Moreover, these mild conditions were extended to differentiated cyclization substrates **3b** (R^1, R^2 = H) and **3c** (R^1 = CF_3, R^2 = H) to generate **4b** (90% yield) and **4c** (86% yield) as single isomers, respectively (entries 7 and 8).

The isomerization of **3a** was explored in detail (Scheme 1). Analysis of a test reaction (*hv* = 300 nm, 0.1 M in THF) by ^{1}H NMR revealed initial isomerization of the exocyclic alkene to generate a mixture of (*E*)-**3a** and (*Z*)-**3a**. These species were present in a 1:1 ratio after 1 h, alongside **4a**. After 2 h, (*E*)-**3a** was consumed and a mixture of (*Z*)-**3a** and **4a** persisted until the reaction was complete. We prepared (*Z*)-**3a** independently and found that the photochemistry of this isomer was indistinguishable from (*E*)-**3a**.[22] Thus, the initial geometry of the exocyclic alkene was inconsequential. In contrast, **4a** did not react with 300 nm light, yet reverted to (*E*)-**3a** in >95% yield when heated to 150 °C *via* a thermal (retro) [1,5]-hydride shift. These results indicate that **4a** is metastable intermediate that likely

Scheme 1. Chromophore disruption in the photoisomerization of **3a** to **4a**.[a]

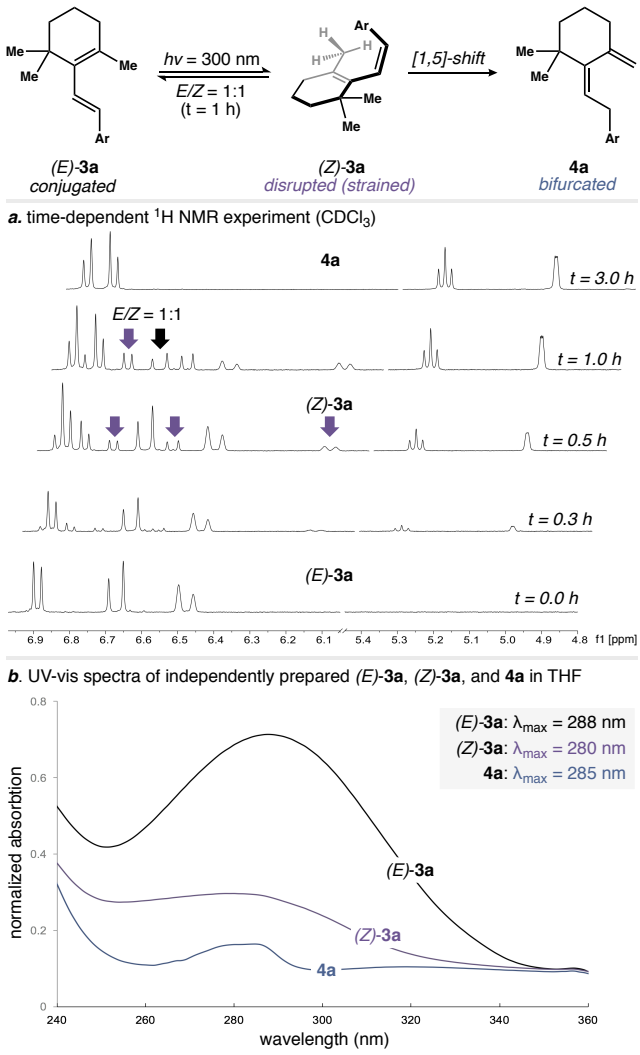

[a] Structure **4a** reverted directly to (*E*)-**3a** at 150 °C.

accumulates because disruption of the extended π-system prevents re-excitation. This conclusion was supported by analyzing the absorption spectra of (*E*)-**3a**, (*Z*)-**3a**, and **4a** in THF. These data revealed significant hypochromic shifts for (*Z*)-**3a** and **4a** relative to (*E*)-**3a**, which is consistent with impaired conjugation. Notably, the π-system in (*Z*)-**3a** is distorted by allylic strain, which also restricts interconversion to the s-trans conformer.[23] This same steric effect may also facilitate a photochemical [1,5]-hydride shift within (*Z*)-**3a** to give **4a**, a process that requires an otherwise difficult-to-achieve antarafacial transition state.[24]

Our next goal was to execute the proposed Heck reaction within **4a**. After some experimentation, we identified the combination of Pd_2dba_3/P(*t*-Bu)$_3$ (1:1 Pd/P) and Cy_2NMe described by Fu to be the most effective.[25] Exposure of **4a** to this catalyst system in dioxane at 85 °C gave **5a** in 93% yield. As shown in Scheme 2, the photoisomerization and Heck cyclization were merged into a single operation. This more convenient process afforded **5a** in 76% yield from **3a** on gram-scale.[26] Moreover, this process was effective across a range of cyclization precursors (**3b**–**3k**). Accordingly, C-ring variants **3b**–**3e** with peripheral substituents at every position around the aryl nucleus were tolerated. By design, a single regioisomer of **5** was obtained in

Scheme 2. Cyclization of β-ionyl substrates **3**: Scope and limitations.[a]

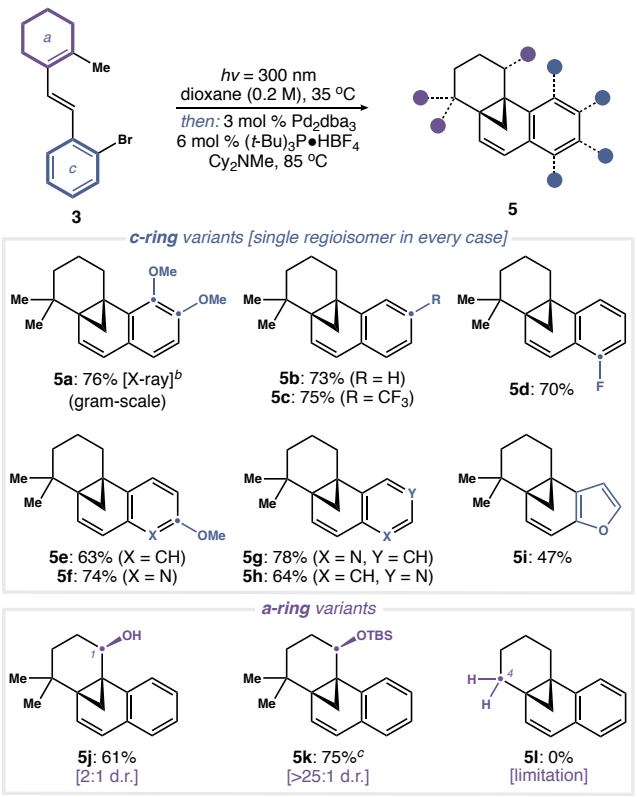

[a] Unless otherwise noted, reactions were carried out on 0.3 mmol scale. Reported yields are based on isolated product after purification. [b] A FEP-tubing spindle was used for the photochemistry (see the Supporting Information for details). [c] Relative stereochemistry was established by single crystal X-ray diffraction.

every case. In addition, the reaction was effective for electron-rich (**5a** and **5e**), non-activated (**5b**), and electron-deficient (**5c** and **5d**) substrates. This feature allowed us to prepare variants of **5** harboring π-deficient (**5f**–**5h**) and π-excessive (**5i**) heterocyclic rings. Modifications of the A-ring were also investigated. For example, the addition of an alcohol at C1 provided **5j** in 2:1 d.r. (61% yield).[27] This selectivity was readily improved to >25:1 d.r. in **5k** (75% yield) when a bulky silyl protecting group was included. In contrast, propellane **5l** lacking a *gem*-dimethyl group at C4 was a limitation. In this case, photolysis of **3l** did not produce isomer **4l**. Instead, $E \rightarrow Z$ isomerization of the exocyclic alkene was the exclusive reaction. This outcome demonstrates the importance of allylic strain introduced by the *gem*-dimethyl group in the [1,5]-hydride shift process.

Having established the proposed photoinduced polycyclization cascade, we turned our attention to examining its utility in target-oriented synthesis. As shown in Scheme 3, we selected abietane diterpenes for this purpose. Our interest in this diterpene family was inspired by taxodione (**8**), a novel inhibitor of farnesyl diphosphate synthase.[28] Among the reported syntheses of **8**,[29] an 11-step route featuring biomimetic polycyclization is the most concise.[30] This work provided a valuable benchmark. We also targeted salviasperanol (**9**), an isomer of **8** distinguished by a [6-7-6] icetexane skeleton.[31] In Nature, this rearranged *abeo*-abietane framework is prepared from an abietane *via* an oxidation-enabled Wagner-Meerwein rearrangement.[32] Nevertheless, **9** is not readily accessible using polyene cyclization. As a result, existing total syntheses of **8** and **9** treat each

Scheme 3. Synthetic entry to common intermediate **11**.

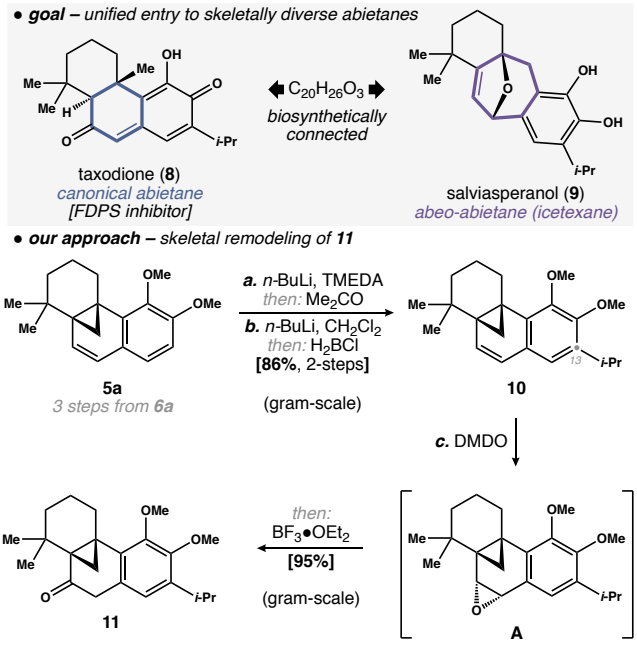

carbocyclic framework as an independent problem.[33]

To evaluate the utility of our strategy, we set out to develop a unified entry point to **8** and **9** *via* late-stage diversification of overbred abietane **11**. This common intermediate was prepared on gram-scale from **5a** *via ortho*-lithiation and trapping with acetone. Deoxygenation of the resultant alcohol using Kabalka's protocol provided **10** in 86% overall yield.[34] The olefin in **10** was then reacted with DMDO to give epoxide **A**, a transient species that smoothly rearranged to ketone **11** in 95% yield upon exposure to $BF_3 \bullet OEt_2$.

A total synthesis of (±)-taxodione (**8**) was achieved from **11** *via* ring-opening of the activated cyclopropyl ketone (Scheme 4). In this case, **11** was reacted with excess TMSCl and NaI in MeCN.[35] Following an aqueous workup, this protocol provided iodide **12** in >95% yield. It was best not to purify this sensitive intermediate. Instead, alkyl iodide **12** was directly reduced with zinc powder to furnish **13** in 82% yield. Deprotection of the aryl ethers with BBr_3 then unveiled the corresponding catechol, which rapidly to oxidized **8** in 93% yield upon exposure to SiO_2 and oxygen.[36] As such, this approach provided (±)-**8** in 9 total steps and 41% overall yield from commercially available fragments **6a** and β-cyclocitral.

Intermediate **11** was also diverted to (±)-salviasperanol (**9**). In this context, alkyl iodide **12** was generated *in situ* as before and then treated with Ag(TFA) to induce a biomimetic skeletal rearrangement.[32] Under dilute conditions (0.05 M), this reaction provided enone **14** in 63% yield alongside an 8:1 mixture of isomers **15a** and **15b**. Mixtures of **15** were recycled to **14** in two steps. In this case, Mukaiyama hydration of **15** gave alcohol **16** as a single diastereomer in 83% yield. Subsequent dehydration of **16** using Burgess reagent (**17**) afforded **14** in 70% yield. Alternatively, a formal synthesis of (±)-**9** was completed by reducing **14** with $LiAlH_4$. Dehydration of the resultant allylic alcohol with **17** furnished diene **18** in 59% yield over two steps. Notably, Sarpong and co-workers previously elaborated **18** to **9**.[33a] Therefore, **9** was formally prepared in 9 total steps (21% overall yield) and, for the first time, along the same synthetic pathway as abietane **8**.

Scheme 4. Diverted total synthesis of (±)-taxodione (**8**) and formal synthesis of (±)-salviasperanol (**9**) from ketone **11**.

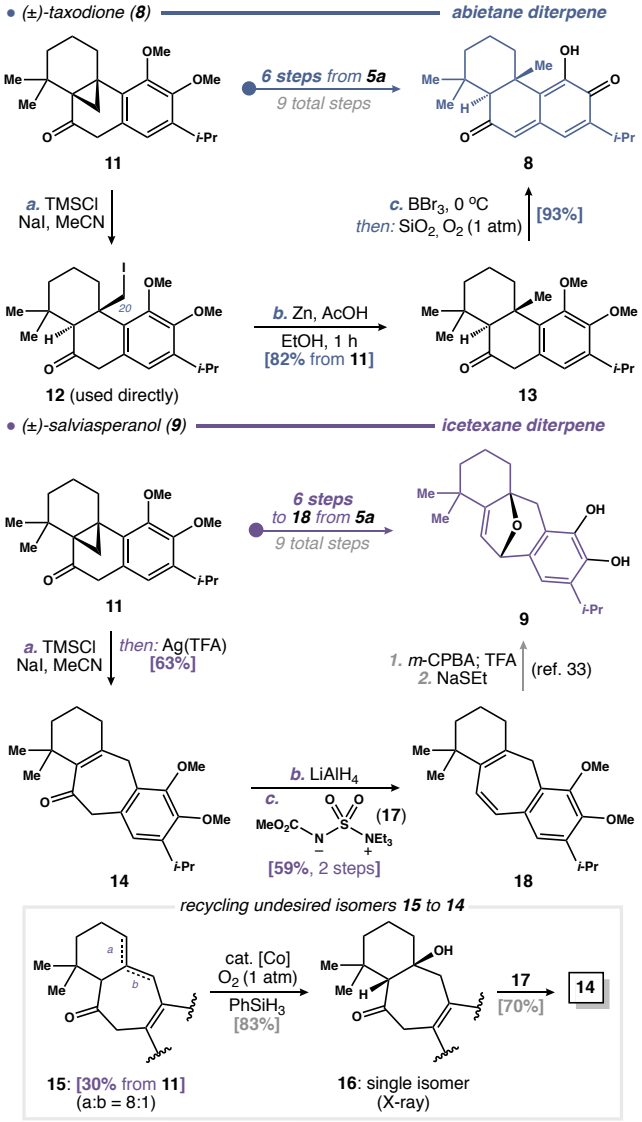

Skeletal remodeling of **11** also supported entry to unprecedented *abeo*-abietane scaffolds (Scheme 5). For example, exposure of **11** to BF_3•OEt_2 in toluene at 80 °C afforded isomeric [6-7-6] ring system **19** in 95% yield. We suspect that that **19** is derived of cation **A**, which itself arises from a (net) [1,3]-alkyl shift within the initial Lewis adduct of **11**.[37] Alternatively, irradiation of **11** ($h\nu$ = 254 nm) in the presence of Et_3N generated [4.4.1] bicyclic motif **20**, putatively *via* ketyl radical **B**.[38] This carbocycle is reminiscent of the cyclocitrinols,[39] and was available at a higher oxidation state from **10**. In this case, **10** was reacted with NIS in aqueous THF to give halohydrin **C**. Upon exposure to Ag(TFA), this reactive species furnished alcohols **21** and **22** in 82% yield (1:1 ratio). We found that **21** isomerized to **22** in the presence of TsOH, putatively *via* cation **D**. Alternatively, **22** was isolated in 82% yield when MeCN was used in place of THF. Collectively, these non-canonical abietanes illustrate the structural diversity that can be achieved by controlled fragmentation of the propellane within **5a**.

In summary, we established an atypical polyene cyclization strategy that converts easily accessible *β*-ionyl derivatives into polycyclic [4.4.1]-propellanes. Unlike canonical biomimetic

Scheme 5. Entry to diversified non-natural *abeo*-abietanes *via* skeletal remodeling of propellanes **10** and **11**.

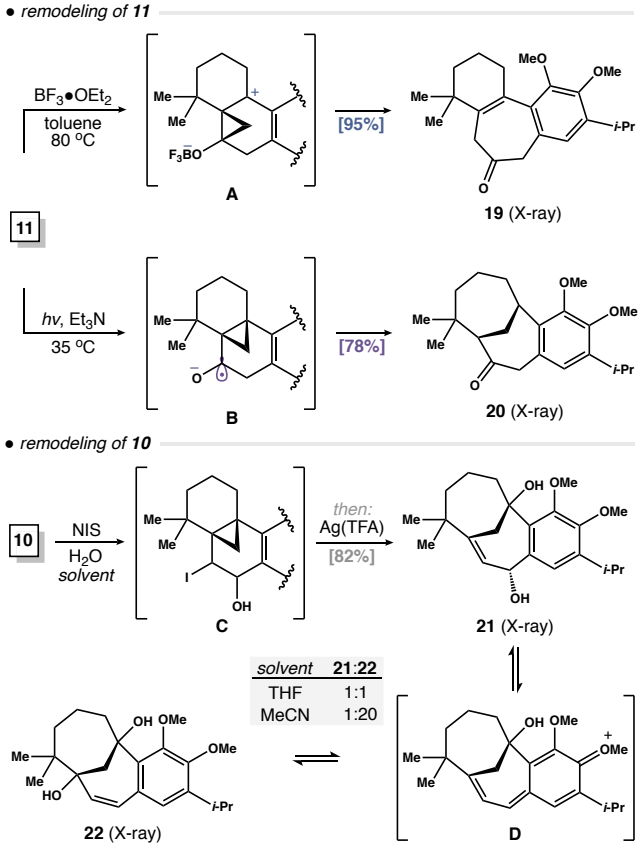

polyene cyclization, this strategy allows for complete control of regiochemistry and tolerates a range of electron-rich and electron-deficient (hetero)aryl groups. The strained polycycles produced from this chemistry were elaborated to diterpene architectures *via* late-stage skeletal remodeling. This powerful feature was highlighted in a unified synthesis of taxodione (**8**) and salviasperanol (**9**) that is concise, modular, and amenable to asymmetric induction in future iterations. Alternative diversification pathways were explored, and these generated a collection of non-canonical *abeo*-abietane scaffolds that would be difficult or impossible to prepare using conventional biomimetic logic. As a result, this terpene assembly strategy appears to be well-suited for applications in both target- and diversity-oriented synthesis.

ASSOCIATED CONTENT

Supporting Information

The Supporting Information is available free of charge on the ACS Publications website.

Experimental procedures, supplemental figures, and characterization data for all new compounds (PDF)

Accession Codes

Supplementary crystallographic data for this paper can be found under the CCDC accession codes: 2129320 (**5a**), 21229321 (**16**), 2129323 (**19**), 2129319 (**20**), 2129322 (**21**), and 2129324 (**22**). These data can be obtained free of charge from the Cambridge Crystallographic Data Centre (CCDC) at www.ccdc.cam.ac.uk.

AUTHOR INFORMATION

Corresponding Author

James H. Frederich – Florida State University, Department of Chemistry and Biochemistry, Tallahassee, FL 32306, United States.
E-Mail: frederich@chem.fsu.edu

Authors

Megan M. Solans – Florida State University, Department of Chemistry and Biochemistry, Tallahassee, FL 32306, United States.
Vitalii S. Basistyi – Florida State University, Department of Chemistry and Biochemistry, Tallahassee, FL 32306, United States.
James A. Law – Florida State University, Department of Chemistry and Biochemistry, Tallahassee, FL 32306, United States.
Noah M. Bartfiled – Yale University, Department of Chemistry, New Haven, CT 06520, United States

Notes

The authors declare no competing financial interest

ACKNOWLEDGMENT

This work was funded by a Florida State University (FSU) Planning Grant (CRC-3425) and, in part, by the NIGMS branch of the NIH under award R01GM125926. We acknowledge Dr. Xinsong Lin (FSU) for his assistance with X-ray crystallography and mass spectrometry. We also thank Professor Joel Smith (FSU) for valuable discussions.

REFERENCES

(1) Cox-Georgian, D.; Ramadoss, N.; Dona, C.; Basu, C. Therapeutic and medicinal uses of terpenes. *Medicinal Plants* **2019**, 333-359.
(2) Newman, D. J.; Cragg, G. M. Natural products as sources of new drugs over the nearly four decades from 01/1981 to 09/2019. *J. Nat. Prod.* **2020**, *83*, 770–803.
(3) Gonzales, M. A. Aromatic abietane diterpenoids: Their biological activity and synthesis. *Nat. Prod. Rep.* **2015**, *32*, 684–704.
(4) Reveglia, P; Cimmino, A.; Masi, M.; Nocera, P.; Berova, N.; Ellestad, G.; Evidente, A. Pimarane diterpenes: Natural source, stereochemical configuration, and biological activity. *Chirality* **2018**, *30*, 1115–1134.
(5) Zhao, X.; Cacherat, B.; Hu, Q.; Ma, D. Recent advances in the synthesis of *ent*-Kaurane diterpenoids. *Nat. Prod. Rep.* **2022**, *39*, 119–138.
(6) (a) Tantillo, D. J. Biosynthesis *via* carbocations: Theoretical studies on terpene formation. *Nat. Prod. Rep.* **2011**, *28*, 1035–1053; (b) Hong, Y. J.; Tantillo, D. J. Formation of Beyerene, Kaurene, Trachylobane, and Atiserene diterpenes by rearrangements that avoid secondary carbocations. *J. Am. Chem. Soc.* **2010**, *132*, 5375–5386.
(7) Dibrell, S. E.; Tao, Y.; Reisman, S. E. Synthesis of complex diterpenes: Strategies guided by oxidation pattern analysis. *Acc. Chem. Res.* **2021**, *54*, 1360–1373.
(8) Zhang, X.; King-Smith, E.; Dong, L.-B.; Yang, L.-C.; Rudolf, J. D.; Shen, B.; Renata, H. Divergent synthesis of complex diterpenes via a hybrid oxidative approach. *Science* **2020**, *369*, 799–806.
(9) For reviews, see: Yoder, R. A.; Johnston, J. N. A case study on biomimetic total synthesis: Polyolefin carbocyclizations to terpenes and steroids. *Chem. Rev.* **2005**, *105*, 4730–4756; (b) Ungarean, C. N.; Southgate, E. H.; Sarlah, D. Enatioselective polyene cyclizations. *Org. Biomol. Chem.* **2016**, *14*, 5454–5467; (c) Barrett, A. G. M., Ma, T.; Mies, T. Recent developments in polyene cyclization and their applications in natural product synthesis. *Synthesis* **2019**, *51*, 67–82; (d) Feilner, J. M.; Haut, F.-L.; Magauer, T. Beyond the isoprene pattern: Bifunctional polyene cyclizations. *Chem. Eur. J.* **2021**, *27*, 7017–7021.
(10) For select examples, see: (a) (c) Ishihara, K.; Nakamura, S.; Yamamoto, H. The first enantioselective biomimetic cyclization of polyprenoids. *J. Am. Chem. Soc.* **1999**, *121*, 4906–4907; (b) Zhao, Y.-J.; Chng, S.-S.; Loh, T.-P. Lewis Acid-promoted intermolecular acetal-initiated cationic polyene cyclizations. *J. Am. Chem. Soc.* **2007**, *129*, 492–493.
(11) For select examples, see: (a) Rendler, S.; MacMillan, D. W. C. Enantioselective polyene cyclization via organo-SOMO catalysis. *J. Am. Chem. Soc.* **2010**, *132*, 5027–5029; (b) Plamondon, S. J.; Warnica, J. M.; Kaldre, D.; Gleason, J. L. Hydrazide-catalyzed polyene cyclization: Asymmetric organocatalytic synthesis of *cis*-decalins. *Angew. Chem., Int. Ed.* **2020**, *59*, 253–258; (c) b) Kutateladze, D. A.; Strassfeld, D. A., Jacobsen, E. N. Enantioselective tail-to-head cyclizaitons catalyzed by dual-hydrogen-bond donors. *J. Am. Chem. Soc.* **2020**, *142*, 6951–6956.
(12) For select examples, see: (a) Sethofer, S. G.; Mayer, T.; Toste, F. D. Gold(I)-catalyzed enantioselective polycyclization reactions. *J. Am. Chem. Soc.* **2010**, *132*, 8276–8277; (b) Schaforth, M. A.; Sarlah, D.; Krautwald, S.; Carreira, E. M. Iridium-catalyzed enantioselective polyene cyclization. *J. Am. Chem. Soc.* **2012**, *134*, 20276–20278; (c) Cochrane, N. A.; Nguyen, H.; Gagne, M. R. Catalytic enantioselective cyclization and C3-fluorination of polyenes. *J. Am. Chem. Soc.* **2013**, *135*, 628–631.
(13) For representative examples of challenges encountered with **1a**, see: (a) Grayfer, T. D.; Retailleau, R.; Dood, R. H.; Dubois, J.; Cariou, K. Chemodivergent, tunable, and selective iodine(III)-mediated bromo-functionalizations of polyprenoids. *Org. Lett.* **2017**, *19*, 4766–4769; (b) Ishihara, K.; Ishibashi, H.; Yamamoto, H. Enantioselective biomimetic cyclization of homo(polyprenyl)arenes. A new entry to (+)-podpcarpa-8,11,13-triene diterpenoids and (–)-tetracyclic polyprenoid of sedimentary origin. *J. Am. Chem. Soc.* **2001**, *123*, 1505–1506.
(14) Electronically deactivated polyenes (e.g. **1b** and **1c**) are challenging substrates for canonical polyene cyclization: (a) Vrubliauskas, D.; Vanderwal, C. D. Cobalt-catalyzed hydrogen-atom transfer induces bicyclizations that tolerate electron-rich and electron deficient intermediate alkenes. *Angew. Chem., Int. Ed.* **2020**, *59*, 6115–6121. (b) Snyder, S. A.; Treitler, D. S. $Et_2SBr{\bullet}SbCl_5Br$: An effective reagent for direct bromonium-induced polyene cyclizations. *Angew. Chem., Int. Ed.* **2009**, *48*, 7899–7903.
(15) Büchi, G.; Yang, N. C. Light-catalyzed organic reactions. VI. The isomerization of some dienones. *J. Am. Chem. Soc.* **1957**, *79*, 2318–2323.
(16) Limura, S.; Overman, L. E.; Paulini, R.; Zakarian, A. Enantioselective total synthesis of guanacastepene N using an uncommon 7-endo Heck cyclization as a pivotal step. *J. Am. Chem. Soc.* **2006**, *128*, 13095–13101.
(17) A creative polycyclization approach to abietane diterpenes was disclosed during the course of this study: (a) Vrubliauskas, D.; Gross, B, M.; Vanderwal, C. D. Stereocontrolled radical bicyclizations of oxygenated precursors enable short syntheses of oxidized abietane diterpenoids. *J. Am. Chem. Soc.* **2021**, *143*, 2944–2952; (b) Johnson, L. K.; Niman, S. W.; Vrubliauskas, D.; Vanderwal, C. D. Stereocontrolled synthesis and structural revision of plebeianol A. *Org. Lett.* **2021**, *23*, 9569–9573.
(18) (a) Naskar, S.; Chowdhury, S. R.; Mondal, S.; Maiti, D. K.; Mishra, S.; Das, I. Visible-light-activated divergent reactivity of dienones: Dimerization in neat conditions and regioselective *E* to *Z* isomerization in solvent. *Org. Lett.* **2019**, *21*, 1578–1582; (b) Livingstone, K.; Tenverge, M.; Pape, F.; Daniliuc, C. G.; Jamieson, C.; Gilmour, R. Photocatalytic $E \rightarrow Z$ isomerization of β-ionyl derivatives. *Org. let.* **2019**, *21*, 9677–9680.
(19) (a) de Mayo, P; Stothers, J. B; Yip, R. W. The irradiation of β-ionone. *Can. J. Chem.* **1961**, *39*, 2135–2137; (b) Ramamurthy, V.; Liu, R. S. H. Sigmatropic hydrogen migration and electrocyclization processes in compounds in the vitamin A series. Photochemistry of polyenes. *J. Org. Chem.* **1976**, *41*, 1862–1867.
(20) Ma, X.; Xu, Q.; Li, H.; Su, C.; Yu, L.; Zhang, X.; Cao, H.; Han, L.-B. Alcohol-based Michaelis-Arbuzov reaction: An efficient and environmentally-benign method for C–P(O) bond formation. *Green Chem.* **2018**, *20*, 3408–3413.
(21) The endoperoxide arising from photooxidation of **3** was formed in the presence of oxygen: Borsarelii, C. D.; Mischne, M.; La Venia,

A.; Vieyra, F. E. M. UVA Self-photosensitized oxygenation of β-ionone. *Photochem. Photobiol.* **2007**, *83*, 1313–1318.
(22) (*Z*)-**3a** was prepared from (*E*)-**3a** using the following procedure: Singh, K.; Staig, S. J.; Weaver, J. D. Facile synthesis of Z-alkenes via uphill catalysis. *J. Am. Chem. Soc.* **2014**, *136*, 5275–5278.
(23) For a similar example, see: Molloy, J. J; Schafer, M.; Weinhold, M.; Morack, T.; Daniliuc, C. G.; Gilmour, R. Boron-Enabled geometric isomerization of alkenes via selective energy-transfer catalysis. *Science* **2020**, *369*, 320–306.
(24) Antarafacial [1,5]-hydride shifts are favored in rare cases: Kiefer, E. F.; Tanna, C. H. Alternative electrocyclic pathways. Photolysis and termolysis of dimethylallene dimers. *J. Am. Chem. Soc.* **1969**, *91*, 4478–4480.
(25) Littke, A. F.; Fu, G. C. A versatile catalyst for Heck reactions of aryl chlorides and aryl bromides under mild conditions. *J. Am. Chem. Soc.* **2001**, *123*, 6989–7000.
(26) We engineered an inexpensive FEP tubing spindle for the purpose of scale up. See the Supporting Information (SI) for details.
(27) The relative stereochemistry of **5j** was confirmed *via* single crystal X-ray diffraction of a C1 alcohol derivative. See the Supporting Information (SI) for details.
(28) (1) Liu, Y.-L.; Lindert, S.; Zhu, W.; Wang, K.; McCammon, J. A.; Oldfield, E. Taxodione and Arenarone Inhibit Farnesyl Diphosphate Synthase by Binding to the Isopentenyl Diphosphate Site. *Proc. Natl, Acad. Sci., USA* **2014**, *111*, E2530–E2539; (b) Han, S.; Li, X.; Xia, Y.; Yu, Z.; Cha, N.; Malal, S. R.; Han, X.; Oldfield, E.; Zhang, Y. Farnesyl pyrophosphate synthase as a target for drug development: Discovery of natural-product-derived inhibitors and their activity in pancreatic cancer cells. *J. Med. Chem.* **2019**, *62*, 10867–10896.
(29) (a) Mori, K.; Matsui, M. Diterpenoid total synthesis XIII: Taxodione, a quinone methide tumor inhibitor. *Tetrahedron* **1970**, *26*, 3467–3473; (b) Matsumoto, T.; Ohsuga, Y.; Harada, S.; Fukui, K. Synthesis of taxodione, royleanone, cryptojaponol, and methyl 11-hydroxy-12-methoxy-7-oxoabieta-8,11)13-trien-18-oate. *Bull. Chem. Soc. Jpn.* **1977**, *50*, 266–272; (c) Matsumoto, T.; Usui, S.; Morimoto, T. A convenient synthesis of (±)-taxodione, (±)-ferruginol, and (±)-sugiol. *Bull. Soc. Chem. Jpn.* **1977**, *50*, 1575–1579; (d) Snitman, D. L.; Himmelsbach, R. J.; Haltwanger, R. C.; Watt, D. S. A synthesis of (±)-cryptojaponol and (±)-taxodione. *Tetrahedron Lett.* **1979**, *20*, 2477–2480; (e) Stevens, R. V.; Bisacchi, G. S. Benzocyclobutenones as synthons for the synthesis of C-11 oxygenated diterpenoids. Application to the total synthesis of (±)-taxodione. *J. Org. Chem.* **1982**, *47*, 2396–2399; (f) Johnson, W. S.; Shenvi, A. B.; Boots, S. G. An approach to taxodione involving biomimetic polyene cyclization. *Tetrahedron* **1982**, *38*, 1379–1404; (g) Poierier, D.; Jean, M.; Burnell, R. H. Alternate syntheses of taxodione. *Synth. Commun.* **1983**, *13*, 201–205; (h) Burnell, R. H.; Jean, M.; Poirier, D. Synthesis of taxodione. *Can. J. Org. Chem.* **1987**, *65*, 775–781; (i) Haslinger, E.; Michl, G. Synthesis of (+)-taxodione from (–)-abietic acid. *Tetrahedron Lett.* **1988**, *29*, 5751–5754; (j) Engler, T. A.; Smapath, U.; Naganathan, S.; Velde, D. V.; Takusagawa, F. A new general synthetic approach to diterpenes: Application to the synthesis of (±)-taxodione and (±)-royleanone. *J. Org. Chem.* **1989**, *54*, 5712–5727.
(30) This total synthesis begins from commercial geranyl chloride and 2-isopropylveratrole: Harring, S. R.; Livinghouse, T. A concise biomimetic total synthesis of (±)-taxodione via a BF_3•$MeNO_2$ promoted cationic cascade annulation. *J. Chem. Soc., Chem. Commun.* **1992**, 502–503.
(31) Simmons, E. M.; Sarpong, R. Structure, Biosynthetic Relationships and Chemical Synthesis of the Icetexane Diterpenoids. *Nat. Prod. Rep.* **2009**, *26*, 1195–1217.
(32) Thommen, C.; Neuburger, M.; Gademann, K. Collective Syntheses of Icetexane Natural Products Based on Biogenic Hypothesis. *Chem. Eur. J.* **2017**, *23*, 120–127.
(33) (a) Simmons, E. M.; Sarpong, R. Ga(III)-Catalyzed Cycloisomerization Strategy for the Synthesis of Icetexane Diterpenoids: Total Synthesis of (±)-Salviasperanol. *Org. Lett.* **2006**, *8*, 2883–2886; (b) Majetich, G.; Zou, G.; Grove, J. Total Synthesis of (±)-Salviasperanol. *Org. Lett*. **2008**, *10*, 85–87.
(34) Yao, M.-L.; Pippin, A. B.; Kabalka, G. W. Deoxygenation of benzylic alcohols using chloroboranes. *Tetrahedron Lett.* **2010**, *51*, 853–855.
(35) Dueterm R. K.; Pounds, S. Ring-opening reactions of electrophilic cyclopropanes. *J. Org. Chem.* **1982**, *47*, 3174–3177.
(36) The unpurified mixture of deprotected **13** was concentrated onto SiO_2, dissolved in $CHCl_3$, and stirred for 1 h under a balloon of O_2. Filtration of the resulting slurry afforded **8** in >95% purity.
(37) In principal, **A** could arise from the initial Lewis adduct of **11** *via* consecutive [1,2] alkyl shifts or a net [1,3] alkyl shift involving a non-classical carbocation: Hong, Y. J.; Giner, J.-L.; Tantillo, D. J. Bicyclobutonium ions in biosynthesis – Interconversion of cyclopropyl-containing sterols from orchids. *J. Am. Chem. Soc.* **2015**, *137*, 2085–2088.
(38) Cossy, J.; Furet, N. Photochemical ring opening of cyclopropyl ketones induced by electron transfer. *Tetrahedron Lett.* **1993**, *34*, 8107–8110.
(39) For an overview of the cyclocitrinols, see: Wu, J.; Liu, J.; Fan, J.-H.; Xie, Z.-D.; Qin, H.; Li, C.-C. Evolution of routes for asymmetric total synthesis of cyclocitrinol enabled by type II [5+2] cycloaddition. *Chin. J. Chem*. **2021**, *39*, 1247–1254.